Proceedings of the Injector MD Days 2017, Geneva, Switzerland, 23 – 24 March 2017, edited by H. Bartosik and G. Rumolo, CERN Proceedings, Vol. 2/2017, CERN-Proceedings-2017-002 (CERN, Geneva, 2017)

SPACE CHARGE AND WORKING POINT STUDIES IN THE CERN LOW ENERGY ION RING

A. Huschauer, H. Bartosik, S. Hancock, V. Kain, CERN, Geneva, Switzerland

INTRODUCTION

The Low Energy Ion Ring (LEIR) is at the heart of CERN's heavy ion physics programme and was designed to provide the high phase space densities required by the experiments at the Large Hadron Collider (LHC). LEIR is the first synchrotron of the LHC ion injector chain and it receives a quasi-continuous pulse of lead ions (Pb^{54+}) from Linac3, exploiting a sophisticated multi-turn injection scheme in both transverse and longitudinal planes. Seven of these pulses are injected and accumulated, which requires continuous electron cooling (EC) at low energy to decrease the phase space volume of the circulating beam in between two injections. Subsequently, the coasting beam is adiabatically captured in two bunches, which are then accelerated and extracted towards the Proton Synchrotron (PS). Figure 1 shows the LEIR magnetic cycle and the different steps required for beam production.

To achieve the ion intensity requirements of the High-Luminosity LHC (HL-LHC), i.e., 8.1×10^8 ions/bunch at LEIR extraction [1, 2], the major LEIR intensity limitation had to be overcome. Past studies showed that up to 50% of the beam was lost after radio-frequency (RF) capture and during the first part of acceleration and, furthermore, the total extracted intensity was reported to be limited to a maximum of 6×10^8 ions/bunch (see dashed line in Fig. 1). Various possible sources limiting the LEIR intensity reach were identified, such as hardware related problems, effects related to direct space charge or collective instabilities of the ion beams [3]. In the framework of the LHC Injectors Upgrade (LIU) project, dedicated studies were started at the end of 2015 to understand the underlying loss mechanism and to find possible mitigation measures. These studies revealed the important interplay of betatron resonances and direct space charge effects during the bunching process [4].

In this paper, the results of more recent experimental and simulation studies, which further emphasize the importance of space charge effects, are summarized and the impact of these studies on the LEIR performance increase is discussed.

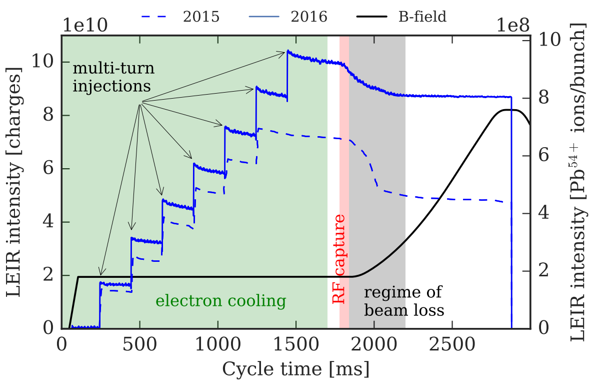

Figure 1: LEIR magnetic cycle of the nominal beam production scheme for heavy ion physics at the LHC. The intensity measurement represented by the solid line corresponds to values that were typically achieved during the 2016 p-Pb LHC run. In earlier years up to 50% of the beam intensity was lost during the first part of acceleration (shown by the dashed line).

CHARACTERIZATION OF THE PERFORMANCE LIMITATION

Figure 2 shows a comparison of the intensity evolution along the LEIR cycle for three different longitudinal phase space distributions. In all three cases the RF voltage functions were programmed such as to perform an iso-adiabatic capture of the coasting beam. The longitudinal emittance of the coasting beam was adjusted prior to RF capture using a periodic modulation of the electron gun voltage. This allowed tailoring the longitudinal emittance of the two bunches after capture. In two cases the beam was captured in single harmonic. The losses clearly decrease with increasing bunching factor (BF), i.e. the average line density divided by peak line density. In other words, enhanced losses are observed for high peak line charge densities. Note that the incoherent tune spread due to direct space charge is directly proportional to the peak line charge density, or inversely proportional to the BF.

RESONANCE IDENTIFICATION STUDIES

In order to characterize resonances close to the operational working point $(Q_{x_0}, Q_{y_0}) = (1.82, 2.72)$, low-intensity tune scans were performed. A single pulse from Linac3 with roughly 2×10^{10} charges was injected and cooled at

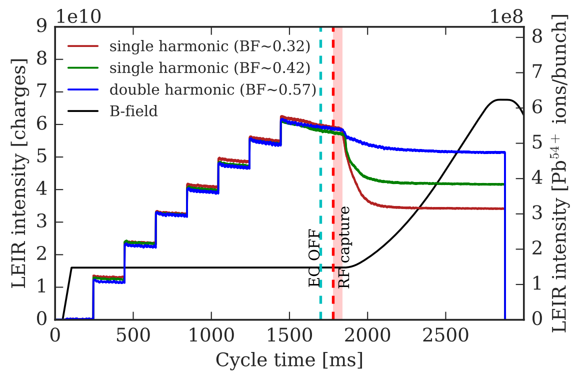

Figure 2: Dependency of beam loss on the longitudinal line density. Losses are significantly reduced for large BFs.

https://doi.org/10.23727/CERN-Proceedings-2017-002.117

these nominal tunes, before the working point was moved to perform the scan. To respect this sequence of events is important for the following two reasons: i) performing a tune scan by changing the tunes at injection is not meaningful as the injection efficiency crucially depends on the tune settings; ii) resonance crossing immediately leads to beam loss in LEIR, which can be significantly mitigated by active EC during the crossing process. Scans with bunched and unbunched beams, which were stored for 500 ms at constant energy, were performed and the beam loss over this period was considered as figure of merit. Figure 3 illustrates the measurement procedure.

This procedure was repeated for multiple working points with bunched and unbunched beams, and the results are shown in Fig. 4. The skew and the normal sextupolar resonances $3Q_y = 8$ and $Q_x + 2Q_y = 7$, respectively, are revealed to be especially strong. In addition, significant beam loss is observed close to the diagonal and the $4Q_y = 11$ resonance for bunched beams. For large horizontal tunes, i.e., $Q_x > 1.9$, beam loss is intrinsic to the way the lattice functions are controlled in LEIR, as the optical β-functions increase drastically. An additional bunched beam tune scan was performed using higher intensity and the corresponding results are shown in Fig. 5. Overall, the same resonance pattern as in Fig. 4 is apparent, but beam loss is significantly increased due to the increased direct space charge tune spread.

An independent way to identify excited resonances is based on the measurement of transverse profiles. In LEIR, horizontal and vertical beam gas ionisation (BGI) profile monitors are available and allow parasitic measurements of the beam size. In order to investigate the effect of the strong skew and normal sextupolar resonances on the beam, the beam size evolution at different working points was studied along the magnetic cycle and the results are shown in

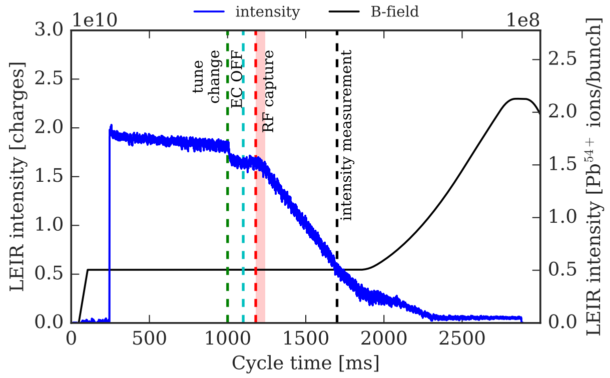

Figure 3: Illustration of the measurement technique for low-intensity tune scans. A single Linac3 pulse was injected at nominal tunes and subsequently cooled. The working point was changed during the EC process to mitigate beam loss when crossing a resonance. Furthermore, the RF capture was advanced by 500 ms with respect to the operational settings.

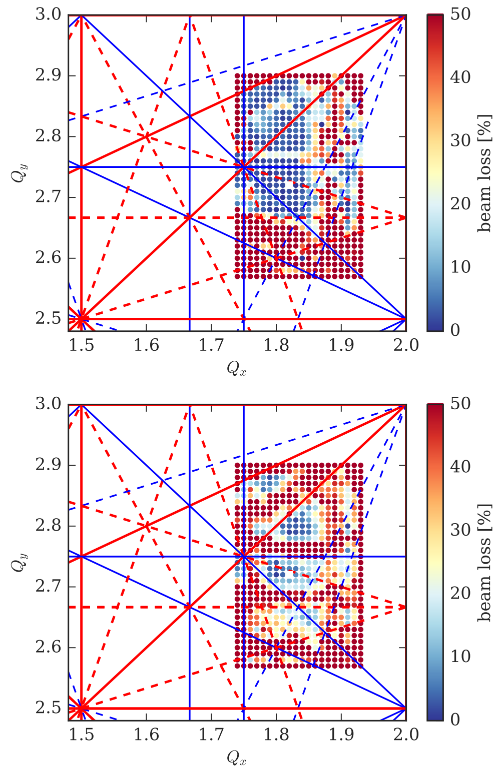

Figure 4: Measured tune diagram in the vicinity of the operational working point (indicated by the white square) for unbunched (top) and bunched beam (bottom). The color scale shows beam loss after 500 ms of storage time. Systematic resonances are shown in red, solid and dashed lines correspond to normal and skew resonances, respectively.

Fig. 6. In addition to the already discussed sextupolar resonances, an effect of the resonance $2Q_x + 2Q_y = 9$ is visible. Furthermore, for decreasing horizontal and vertical tunes, the horizontal beam size experiences a significant growth, possibly due to the resonance $4Q_x = 7$.

The driving term of these resonances remains unknown today. The presence of the electron cooler and its multitude of magnetic elements was expected to significantly contribute to the excitation of resonances. Therefore, an additional study using the bare machine was performed. To perform this test, the main solenoid of the electron cooler as well as the corrector solenoids, all additional magnetic elements of the cooler, the correction of the orbit distortion around the electron cooler and all chromatic and harmonic sextupoles were switched off.

Using this configuration, the skew sextupolar resonance $3Q_y = 8$ was crossed and no significant differences in terms of beam loss when crossing the resonances were observed (see Fig. 7). Therefore, the electron cooler was excluded as source of skew sextupolar errors and a possible source is yet to be determined. Furthermore, the normal sextupolar resonances are expected to be excited by magnetic errors in the main bending dipoles.

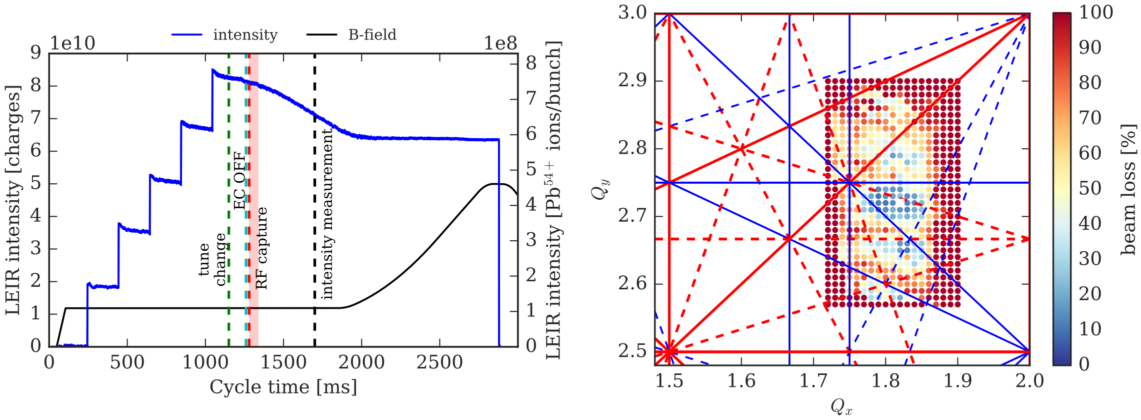

Figure 5: Measured high-intensity tune diagram for bunched beam. Left: Illustration of the measurement technique likewise to Fig. 3. Right: Measurement results in the vicinity of the operational working point (indicated by the white square). The resonance pattern is very similar to the one observed in Fig. 4.

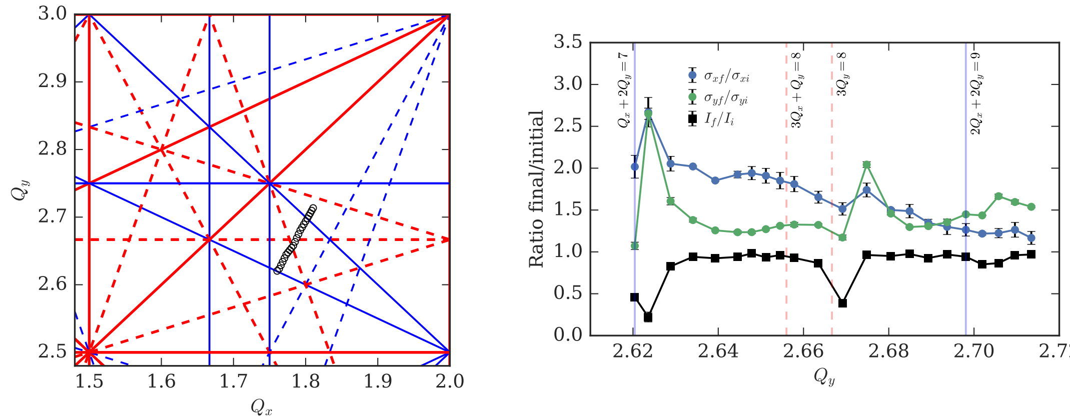

Figure 6: For each working point indicated in the tune diagram on the left, the ratio between final and initial beam sizes for each transverse plane and the corresponding intensity are shown on the right. The observed shift between maximum blow-up and theoretical position of resonance lines (blue and red vertical lines in the background) is compatible with the maximum direct space charge tune spread $\Delta Q_x \approx \Delta Q_y \approx -3 \times 10^{-2}$. The error bars correspond to the statistical fluctuations over three consecutive measurements.

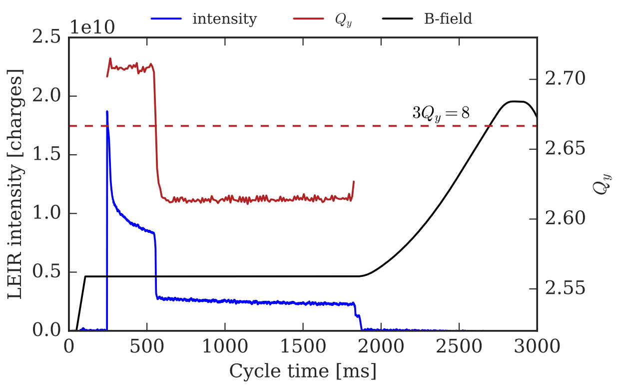

Figure 7: Also in the absence of the magnetic effects of the electron cooler, significant beam losses are observed when crossing the resonance $3Q_y = 8$. The significant drop of intensity right after injection is due to the large beam size in the absence of EC.

Given the fact that the direct space charge tune spread $\Delta Q_{x,y}$ of operational beams reaches values larger than 0.1 during the RF capture process (see also [4]), particles experience the effect of multiple resonances simultaneously, which might lead to emittance blow-up and beam loss at the main aperture restriction of LEIR, i.e., the vacuum chambers inside the bending magnets. Therefore, additional studies, which are presented in the following, were performed to compensate or avoid the resonances. The latter can be achieved by modification of the machine optics.

RESONANCE COMPENSATION

With the current operational setup of LEIR, it is essential to control the transverse tunes precisely. One possible means to relax this constraint is to compensate resonances, which can be attempted by using either the eight installed chromatic or the two harmonic sextupoles. In fact, the latter are a combination of normal and skew sextupoles in a single element.

A first proof of principle has been presented in [4], where a reduction of the current in the chromatic sextupoles was observed to lead to reduced beam loss close to the resonances. Subsequently, a more systematic approach was pursued: using the Polymorphic Tracking Code (PTC [5]) library inside MAD-X [6], the resonance driving terms (RDTs) of the different sextupoles were computed and suitable pairs of sextupoles for compensation studies were determined (see Fig. 8). The feasibility of compensation with several of these pairs was then studied by programming the working point to lie on top of the $Q_x + 2Q_y = 7$ resonance, while scanning the current in the sextupoles and recording beam loss simultaneously. The results are shown in Fig. 9: for any combination of two chromatic sextupoles, but also by using one chromatic and one harmonic sextupole, resonance compensation can be achieved for certain currents. Surprisingly, however, no compensation could be achieved by using the pair of harmonic sextupoles, even though their functionality has been verified. This issue will be further investigated in the future. In Fig. 10 the results from Fig. 9 are displayed in a different way, namely by transforming the measured sextupole currents into the RDT-space. As expected, the phase and amplitude of the resonance, which corresponds to the area of maximum beam survival, is observed to be identical for different combinations of sextupoles.

In addition, the impact of resonance compensation on the evolution of the transverse profiles was studied. A low-intensity beam was injected, cooled and stored with active resonance compensation (corresponding to the optimum settings found for the scan using SXFN11 and SXFN32 in Fig. 9) for several hundreds of milliseconds. Subsequently, the compensating sextupoles were switched off during the cycle and the evolution of the beam size during the entire magnetic cycle was recorded using the BGI monitor. In Fig. 11, the suppressed growth of the beam size during the first part of the cycle is clearly visible.

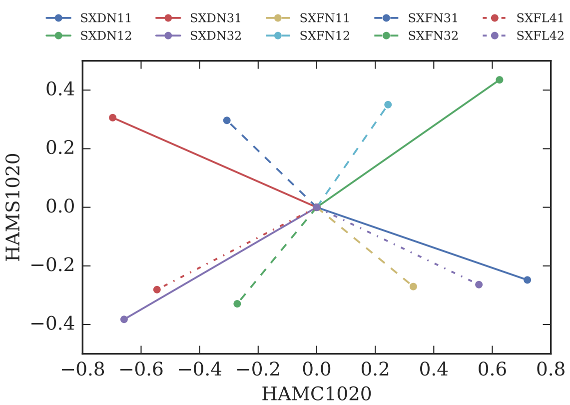

Figure 8: Hamiltonian RDTs for the different sextupoles installed in LEIR. Pairs of sextupoles whose vectors are at an angle of 90 degrees are well suited elements for compensation.

OPERATION AT A DIFFERENT WORKING POINT

The LEIR machine optics configurations are significantly constrained by the multi-turn injection and EC processes [7–9]. In order to modify the lattice optics and move the working point to a quadrant of the tune diagram that is less resonance dominated, a dedicated simulation study was performed and a suitable stable solution was obtained for the tunes $(Q_x, Q_y) = (2.18, 3.28)$. In Fig. 12, the optics functions for both setups are compared and the main difference concerns the β_y-functions at the entrance and exit of the bending magnets. Considering this fact, the optics modification is clearly unfavorable. However, if the overlap between the direct space charge tune spread and excited resonances is significantly reduced, emittance growth during the RF capture is also expected to be mitigated, resulting in an overall reduction of beam loss.

To investigate the resonance excitation in this new optics configuration, an additional measurement was performed. The result is shown in Fig. 13 and the resonance free area is found to be significantly increased compared to the measurements in the nominal configuration (see Fig. 2).

The continuation of the optimization of this new machine setup and the investigation of transverse emittance blow-up and beam loss are subject of future studies.

CONCLUSIONS AND OUTLOOK

The early part of LEIR operation in 2016 was fully dedicated to deepening the understanding of the performance limitations and to investigating mitigation possibilities. The combination of the results presented in this paper in combination with the excellent performance of Linac3 [10], and additional modifications of the RF capture process [11], led to the unprecedented Pb^{54+}-intensity of more than 10^{10} charges at LEIR extraction (see Fig. 14). Therewith, the HL-LHC ion intensity requirement has been operationally demonstrated in LEIR and the major remaining challenge is to maintain this high performance of the machine and Linac3, and to reduce the sensitivity of the performance to the various machine settings by exploiting resonance compensation or the modified optics configuration. Furthermore, the reduction of the time between two subsequent injections into LEIR and operation with increased electron current in the cooler is being studied to increase the accumulated intensity and provide more margin for future operation [12].

REFERENCES

[1] J. Coupard *et al.* (eds.), "LHC Injectors Upgrade, Technical Design Report, Vol. II: Ions", CERN-ACC-2016-0041 (2016).

[2] H. Bartosik *et al.*, "The LHC Injectors Upgrade (LIU) Project at CERN: Ion Injector Chain", Proc. of IPAC'17, Copenhagen, Denmark (2017), TUPVA020, pp 2089-2092.

[3] M.A. Bodendorfer, M.E. Angoletta, J. Axensalva,D. Manglunki, and S. Pasinelli, "Beam Loss in the Low Energy Ion Ring (LEIR) in the Light of the LHC Injectors Upgrade for

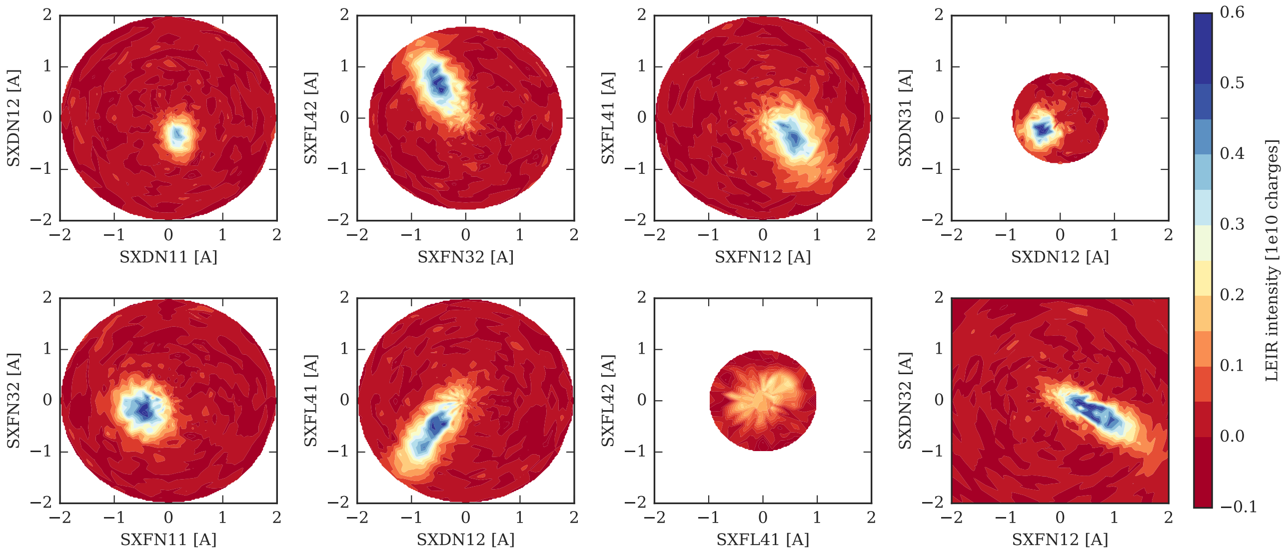

Figure 9: Beam survival after 600 ms of storage time as a function of current in the sextupoles. A combined use of harmonic (SXFL*) and chromatic (SXFN*/SXDN*) sextupoles clearly reveals reduced resonance excitation. Contrary to expectations, no such effect can be observed by using pairs of harmonic sextupoles only.

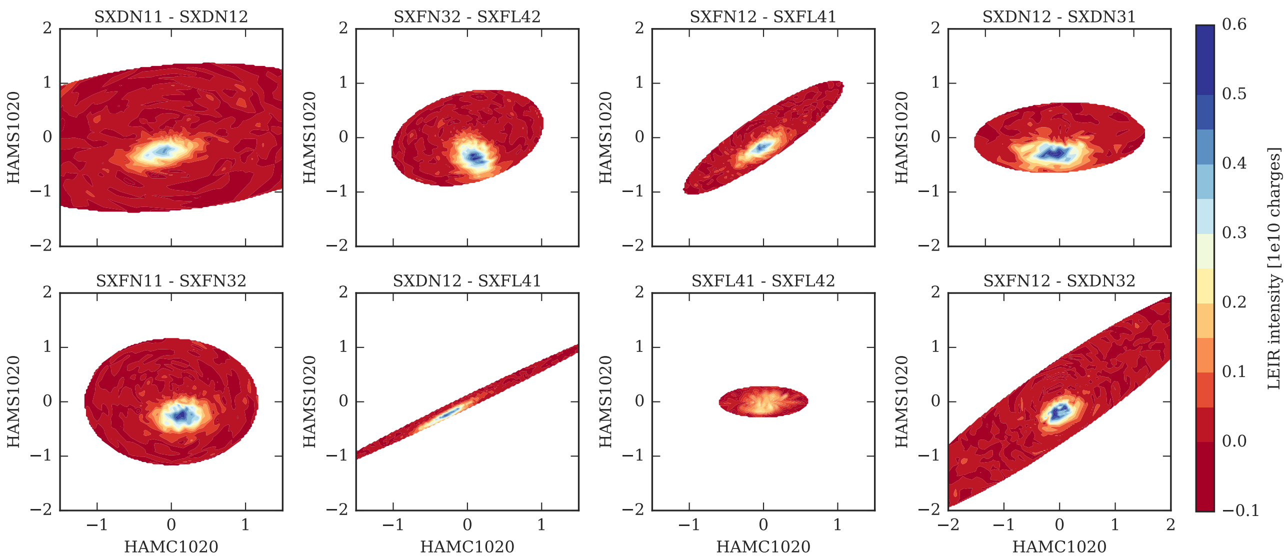

Figure 10: Measurement results of Fig. 9 transformed into RDT-space. Amplitude and phase of the resonance are in very good agreement for the different scans.

Ions (LIU-Ions)", in *Proc. of HIAT15*, Yokohama, Japan (2015), pp. 115-117.

[4] H. Bartosik, S. Hancock, A. Huschauer, and V. Kain, "Space Charge Driven Beam Loss for Cooled Beams and Mitigation Measures in the CERN Low Energy Ion Ring", in *Proc. of HB2016*, Malmö, Sweden (2016), pp. 272–277.

[5] F. Schmidt, E. Forest, and E. McIntosh, "Introduction to the polymorphic tracking code: Fibre bundles, polymorphic Taylor types and "Exact tracking", CERN-SL-2002-044-AP, KEK-REPORT-2002-3 (2002).

[6] W. Herr and F. Schmidt, "A MAD-X Primer", CERN-AB-2004-027-ABP (2004).

[7] M. Benedikt, P. Collier, V. Mertens, J. Poole, and K. Schindl (eds.),"LHC Design Report", Volume III, Chapter 35, CERN, Geneva, Switzerland (2004).

[8] C. Carli, S. Maury, and D. Mohl, "Combined longitudinal and transverse multiturn injection in a heavy ion accumulator", in *Proc. of PAC97*, Vancouver, Canada (1997), pp. 976-978.

[9] J. Bosser, C. Carli, M. Chanel, R. MacCaferri, S. Maury, D. Möhl, G. Molinari, G. Tranquille, "Electron cooling of PB^{54+} ions in the low energy ion ring (LEIR)", in *Proc. of EPAC98*, Stockholm, Sweden (1998), pp. 1073-1075.

[10] G. Bellodi, "Source and Linac3 studies'", elsewhere in these proceedings.

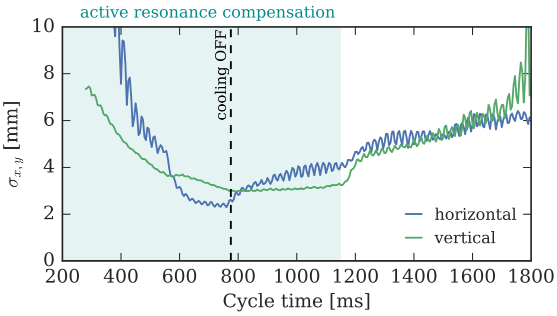

Figure 11: Impact of resonance compensation on the evolution of the horizontal and vertical beam sizes, σ_x and σ_y, respectively. Once the sextupoles are switched off, the beam immediately grows in both transverse planes.

[11] S. Albright *et al.*, “LEIR Longitudinal dynamics studies”, elsewhere in these proceedings.

[12] R. Scrivens *et al.*, “100 ms injection into LEIR”, elsewhere in these proceedings.

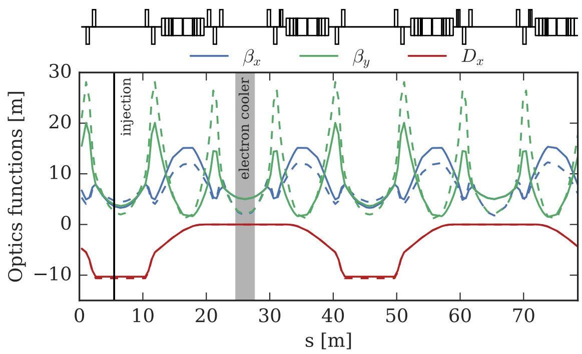

Figure 12: LEIR optics functions for the nominal (solid lines) and modified (dashed lines) settings.

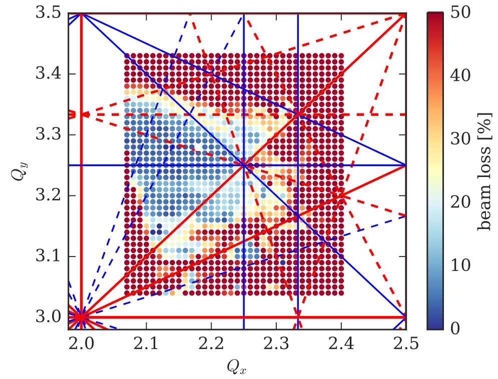

Figure 13: Measured tune diagram for the modified LEIR optics configuration. The design working point for this machine setup is indicated by the white square.

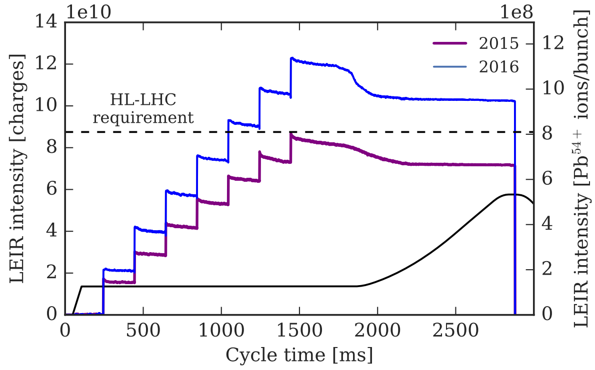

Figure 14: In 2016, the extracted intensity out of LEIR was increased by 40% compared to the performance at the end of 2015.